SAND2011-5086C

A Statistical Method for Verifying Grid and Mesh Convergence in Direct Monte Carlo Simulations

Joseph Bishop[1] and Erik Strack[2]

[1]Computational Structural Mechanics
Sandia National Laboratories
Albuquerque, NM

[2]Computational Shock and Multiphysics
Sandia National Laboratories
Albuquerque, NM

Presented at the 11th U.S. National Congress on Computational Mechanics
Minisymposium on Adaptive Methods for Uncertainty Quantification
July 25-28, 2011,

This material is based upon work supported as part of the Center for Frontiers of Subsurface Energy Security, an Energy Frontier Research Center funded by the U.S. Department of Energy, Office of Science, Office of Basic Energy Sciences under Award Number DE-SC0001114.

Sandia is a multi-program laboratory operated by Sandia Corporation, a Lockheed Martin Company, for the United States Department of Energy's National Nuclear Security Administration under Contract DE-AC04-94AL85000.

Outline

1. Deterministic horizon in nonlinear dynamical systems (sensitivity to initial conditions)
2. Example: contact-impact system (bouncing ball)
3. Assessing mesh convergence beyond the deterministic horizon (KS statistic)
4. Example: ductile ring fragmentation
5. Optimal sample sizes
6. Summary

Deterministic Horizon

- result of extreme sensitivity to initial conditions
- inherent to the math/physics, not numerical scheme

trajectories in phase space

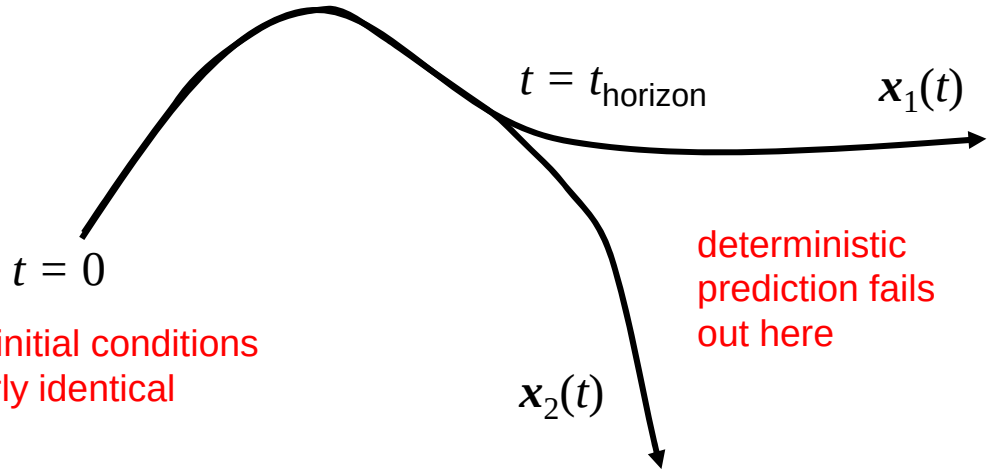

$$\boldsymbol{\delta}(t) = \boldsymbol{x}_1(t) - \boldsymbol{x}_2(t)$$

$$\|\boldsymbol{\delta}(t)\| \sim \|\boldsymbol{\delta}_0\| e^{\lambda t}$$

$$t_{\text{horizon}} \sim O\left(\frac{1}{\lambda} \ln \frac{a}{\|\boldsymbol{\delta}_0\|}\right)$$

λ = Liapunov exponent

a = acceptable accuracy

Sandia National Laboratories

Example: A Contact-Impact System, (Bouncing Ball)

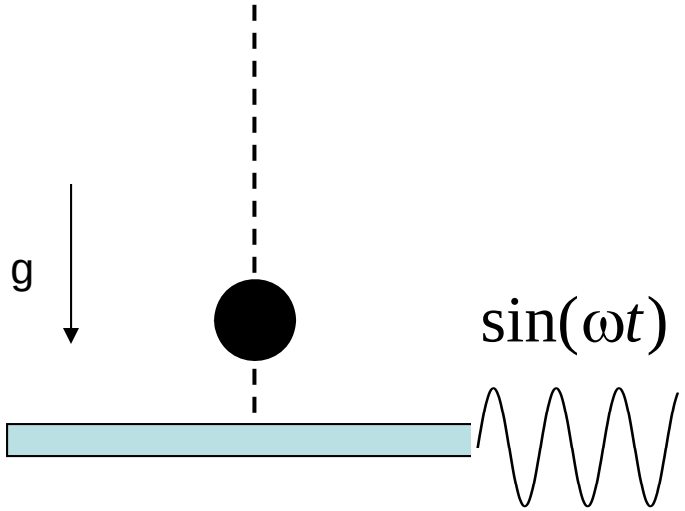

1 degree of freedom (up and down)

initial drop height

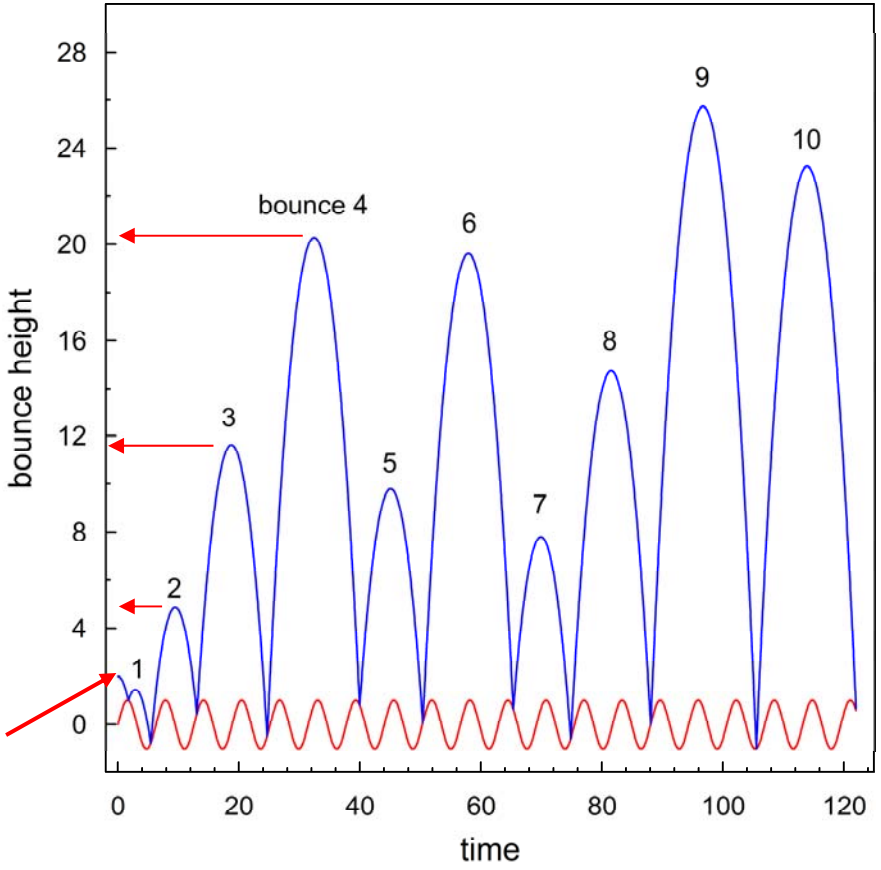

Sandia National Laboratories

Height between Bounces

bounce 1,2,3, and 4

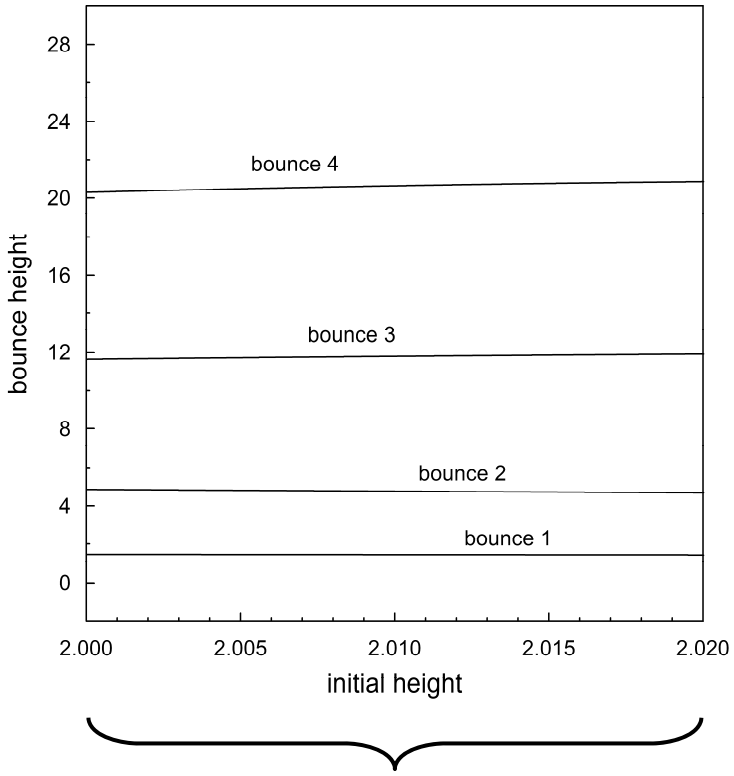

bounce 5,6, and 7

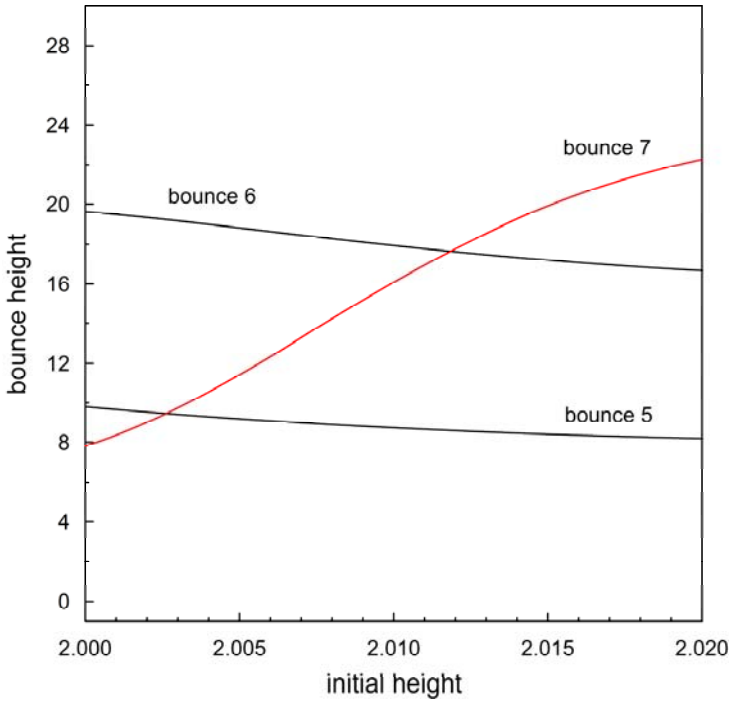

1% variation on initial height

Sandia National Laboratories

Height between Bounces

bounce 8 and 9

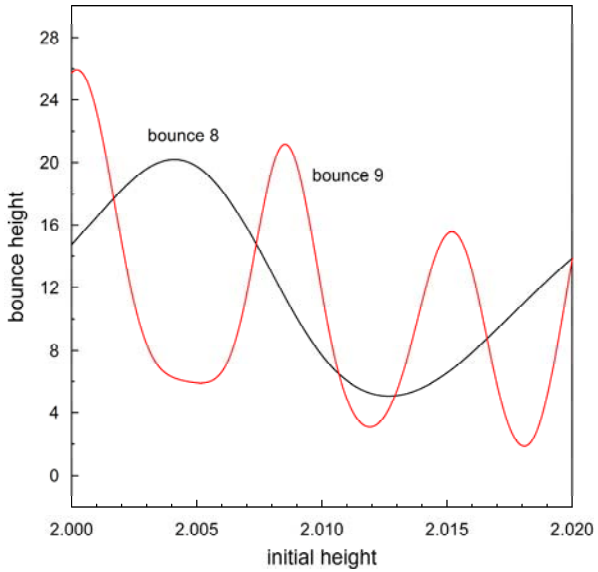

bounce 10

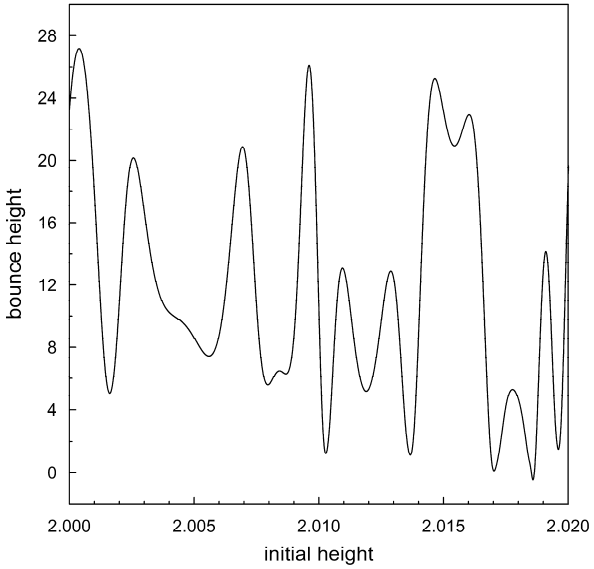

bounce 11

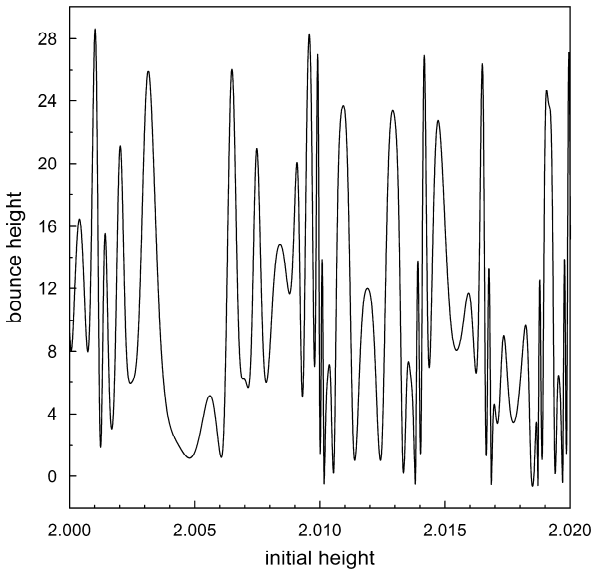

- Each bounce stretches and folds phase space (position and velocity).
- Correlation of bounce height with input height decreases with each bounce.
- Information is lost (entropy is created) with each bounce.
- There exists a deterministic time-horizon beyond which only a statistical description is possible.

Sandia National Laboratories

What about a Polynomial-Chaos Expansion?

- Assume we have a uniform distribution on the initial drop height.
- Optimal basis is the Legendre chaos.

$$H(h) = \sum_{i=0}^{N} H_i \, \varphi_i(\xi)$$

$\varphi_i(\xi)$ Legendre polynomials

$$\varphi_0(\xi) = 1 \qquad -1 \le \xi \le 1$$

$$\varphi_1(\xi) = \xi$$

$$\varphi_2(\xi) = \frac{1}{2}\left(3\xi^2 - 1\right)$$

$$\varphi_3(\xi) = \frac{1}{2}\left(5\xi^3 - 3\xi\right)$$

$$\vdots$$

bounce	PC order
1-4	1
5	2
7	3
8	4
9	8
10	>20
11	>40
12	>80

Required PC order doubles with each bounce.

Sandia National Laboratories

Nonlinear Dynamical Systems

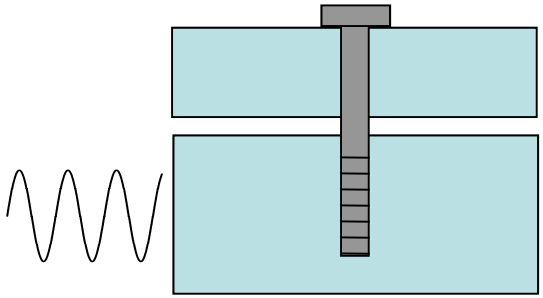

piecewise-smooth dynamical systems

- stick-slip
- contact-impact

buckling

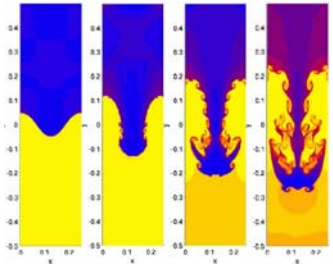

Rayleigh-Taylor instability

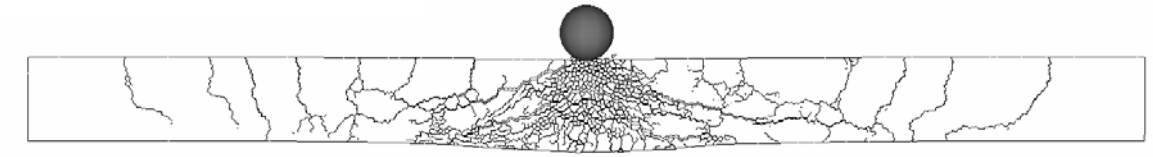

pervasive fracture

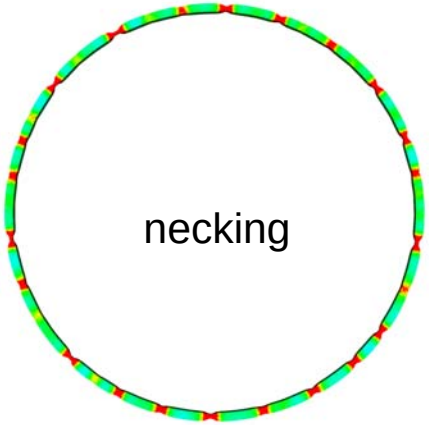

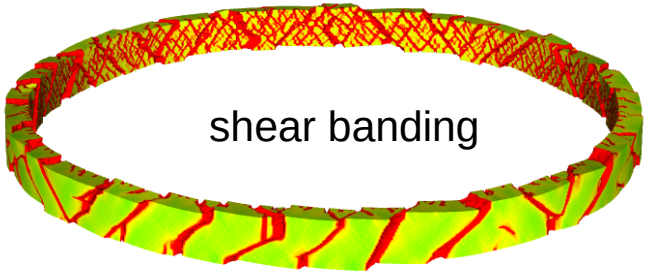

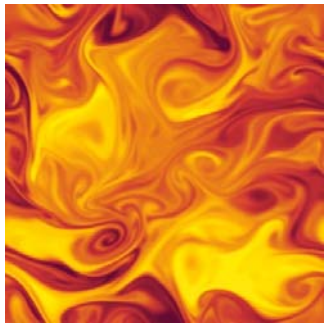

turbulence

These deterministic systems exhibit extreme sensitivity to initial conditions and system parameters.

Example: Ductile Thin Ring Expansion

Grady, D. and D. Benson (1983). "Fragmentation of metal rings by electromagnetic loading." Experimental Mechanics 23(4): 393-400.

Fragmentation of Metal Rings by Electromagnetic Loading

Fragmentation studies on rapidly expanding metal rings are performed with electromagnetic loading. Dynamic-fracture strain and fragment-size measurements are reported for aluminum and copper

by D.E. Grady and D.A. Benson

ABSTRACT—A method is described for performing fragmentation studies on rapidly expanding metal rings. A fast-discharge capacitor system generates magnetic forces which accelerate the rings to maximum radial velocities of approximately 200 m/s corresponding to circumferential-strain rates of approximately $10^4/s$ at fragmentation. Streak-camera techniques are used to record the time-resolved motion of the rings. Fracture-strain and fragmentation experiments have been performed on samples of OFHC copper and 1100-0 aluminum.

Introduction

The fragmentation of a body due to a violent impulsive load is a complicated phenomenon which currently cannot be calculated with confidence. Dynamic loading leads to myriad interactions of stress waves which govern the fragmentation event. In addition, material-property effects and statistics of the fracture nucleation and growth process are also important.

Interpretation of dynamic-fracture experiments is complicated by the multiaxial and heterogeneous stress states occurring in most impact- or explosive-loading studies. Consequently, experimental methods which simplify the stress conditions leading to fragmentation of the body offer a better possibility of understanding the principles governing dynamic fragmentation. One attractive method is provided by radial loading of ring-shape specimens with magnetic forces in which dynamic fracture and fragmentation is brought about by the rapid application of a homogeneous one-dimensional tensile stress. The present report describes such radial-loading fragmentation experiments. Data on ring samples of 1100-0 aluminum and OFHC copper are also provided.

The expansion of rings and cylindrical shells has been used productively in the past to investigate the phenomenon of dynamic deformation. Numerous studies by direct application of explosive loading to the interior wall of cylindrical samples have been made. The method is extremely energetic, however. Experimental control is complicated by the explosive violence, product gases, and preconditioning of samples through application of the initial high-amplitude shock wave. An improved laboratory technique has been explored[1-3] where the sample ring is isolated from the explosive by a cylindrical, high-strengh metal mandrel. Recently, Warnes *et al.*[4] have extended this technique and used velocity interferometry to determine time-resolved motion of the expanding ring. Again, there is concern about shock preconditioning of the sample. Shock-wave studies indicate that material properties in metals can be severely altered by shock stresses above approximately 10 GPa.[5,6] Also, the impulse provided by this method is not sufficient to produce significant fragmentation.

The application of magnetic forces to load ring or cylindrical geometries appears to have been described in the literature first by Niordson.[7] A similar system has been described by Walling and Forrestal[8] and used by Wesenberg and Sagartz[9] to conduct fragmentation studies on large aluminum cylinders, illustrating the energy capability of this technique. Magnetic loading has several attractive features: (1) motion is imparted to the sample through continuous body forces rather than shock loading and consequently, preconditioning shock effects are eliminated; (2) loading rates are readily controlled through variation in rate and amplitude of the driving-current pulse; and (3) the method is more conducive to a laboratory environment than explosive-loading schemes. A magnetic-loading technique is not without its drawbacks, however. Since it is based on the principle of opposing forces between primary and induced currents, inductive heating, which may also have preconditioning effects, can occur in the sample material. Also, when fragmentation occurs, arcing of induced currents can result in additional local-heating effects.

The system that we have developed to conduct fragmentation experiments on metal rings is modest compared to the 250-kJ fast-discharge capacitor system described by Walling and Forrestal.[8] The present method uses approximately 10 kJ of energy and compares most closely to the work described by Niordson.[7] Implementation of the technique required additional development, however, and consequently, some description is warranted. For example, smaller experimental assemblies were found to be more sensitive to loading instabilities and different techniques were needed to apply the magnetic forces. The method

D.E. Grady and D.A. Benson are Research Scientists, Sandia National Laboratories, Albuquerque, NM 87185.

Original manuscript submitted: March 29, 1982. Final version received: July 11, 1983.

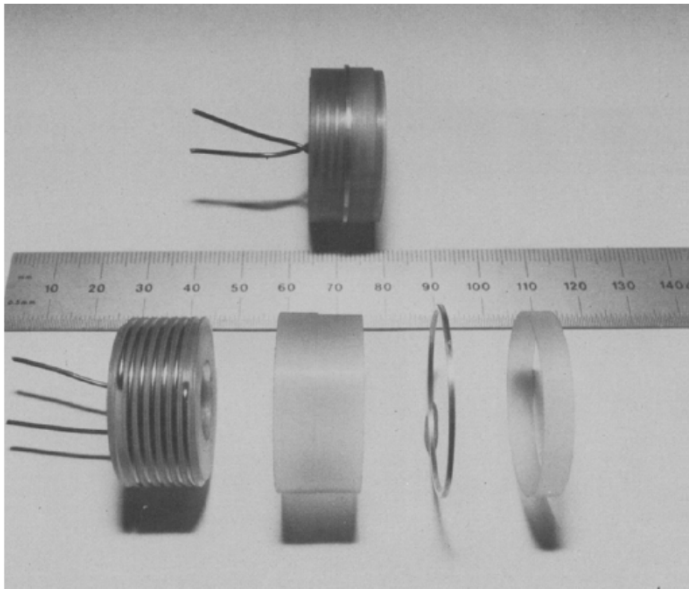

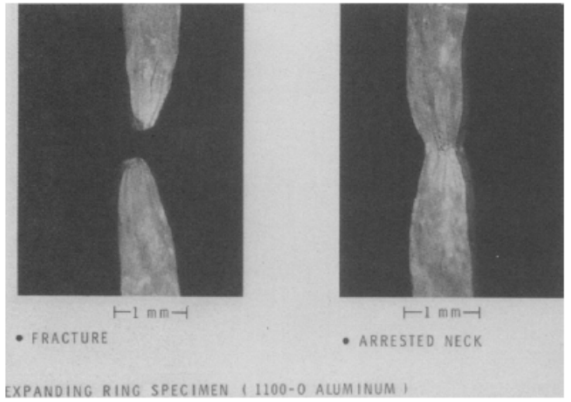

Fig. 5—Photograph of fracture and arrested-neck region from dynamic expansion of an aluminum ring

Sandia National Laboratories

International Journal of Impact Engineering 35 (2008) 1661–1665

Contents lists available at ScienceDirect

International Journal of Impact Engineering

journal homepage: www.elsevier.com/locate/ijimpeng

CTH simulations of an expanding ring to study fragmentation

J.P. Meulbroek [a,*], K.T. Ramesh [a], P.K. Swaminathan [b], A.M. Lennon [b]

[a] Johns Hopkins University, 3400 North Charles Street, Baltimore, MD, USA
[b] Johns Hopkins Applied Physics Laboratory, 11100 Johns Hopkins Road, Laurel, MD, USA

ARTICLE INFO

Article history:
Available online 3 August 2008

Keywords:
Fragmentation
Expanding ring
Ductile failure
Void growth
Simulations

ABSTRACT

A high velocity impact will result in fragmentation which can be seen through EO/IR/RF signatures. Understanding fragmentation and how it relates to signatures is key to being able to characterize the impact. To study fragmentation in a computational context, an expanding ring was simulated using the shock physics hydrocode CTH. The simulations were set up to approximate the conditions of experiments performed by Zhang and Ravi-Chandar [On the dynamics of necking and fragmentation – I. Real-time and post-mortem observations in Al 6061-O. Int J Fract 2006;142:183–217]. The simulations resulted in random fragmentation patterns that are mesh size dependent. The simulations could not capture either the fragment sizes and distributions or the physics of the failure mechanism seen in experiments. The mechanics of failure represented in the simulations is extremely sensitive to the material model and how damage is treated in that model. However, the average fragment size in the simulations versus strain rate was found to be consistent with popular fragmentation models such as Grady–Kipp and Zhou–Molinari–Ramesh.

"The simulations resulted in random fragmentation patterns that are mesh size dependent."

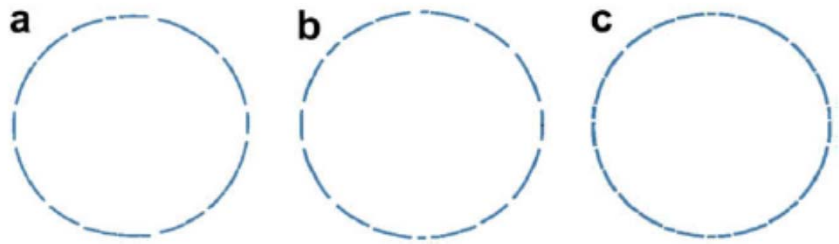

Fig. 4. Fragmentation patterns for three different meshes. (a) Coarse mesh with 7.5 elements through the thickness. (b) Medium mesh with 10 elements through the thickness. (c) Fine mesh with 15 elements through the thickness.

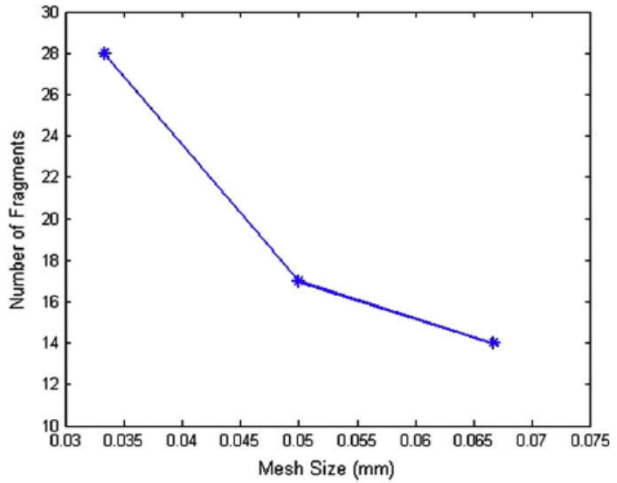

Fig. 5. Number of fragments versus mesh size. For three different mesh sizes, three different fragmentation patterns emerged showing that fragmentation is mesh dependent.

Definitions of Statistical Convergence

X engineering quantity of interest, a random variable

X_h random variable for a given mesh resolution h

F_h cumulative distribution for a given mesh resolution h

Almost Sure Convergence

$$\Pr\left(\lim_{h\to 0} X_h = X\right) = 1 \quad \text{a.e.}$$

Convergence in r-mean

$$\lim_{h\to 0} E\left[\left|X_h - X\right|^r\right] = 0$$

Convergence in Probability

$$\lim_{h\to 0} \Pr\left(\left|X_h - X\right| > \varepsilon\right) = 0$$

increasing strength

Convergence in Distribution

$$\lim_{h\to 0} F_h(x) = F(x)$$

Sandia National Laboratories

How to Assess Convergence in Distribution?

$$\lim_{h \to 0} F_h(x) = F(x)$$

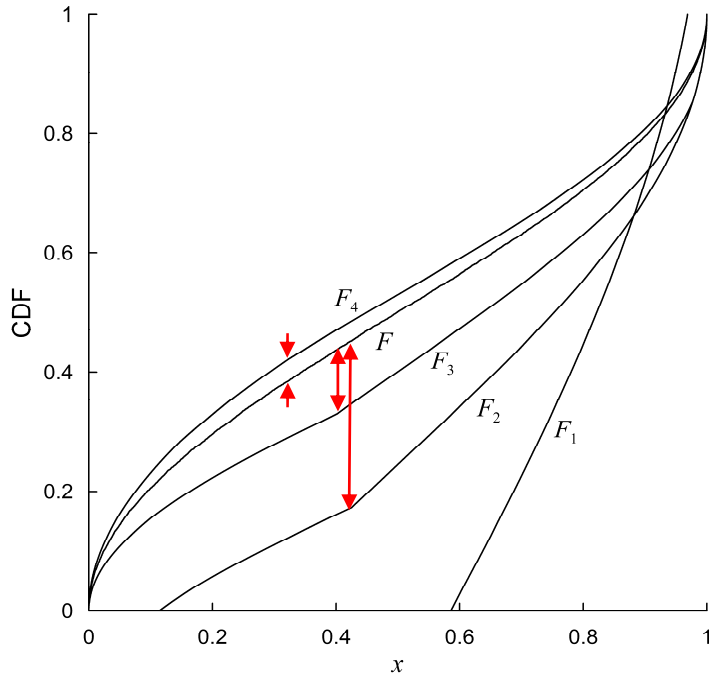

use L_∞ norm: $L_\infty(F_h, F) = \sup_x |F_h(x) - F(x)|$

To have a complete function space with this norm, need to assume F_h is continuous.

(Space of continuous functions is complete in the L_∞ norm.)

Sandia National Laboratories

What about finite sampling effects?

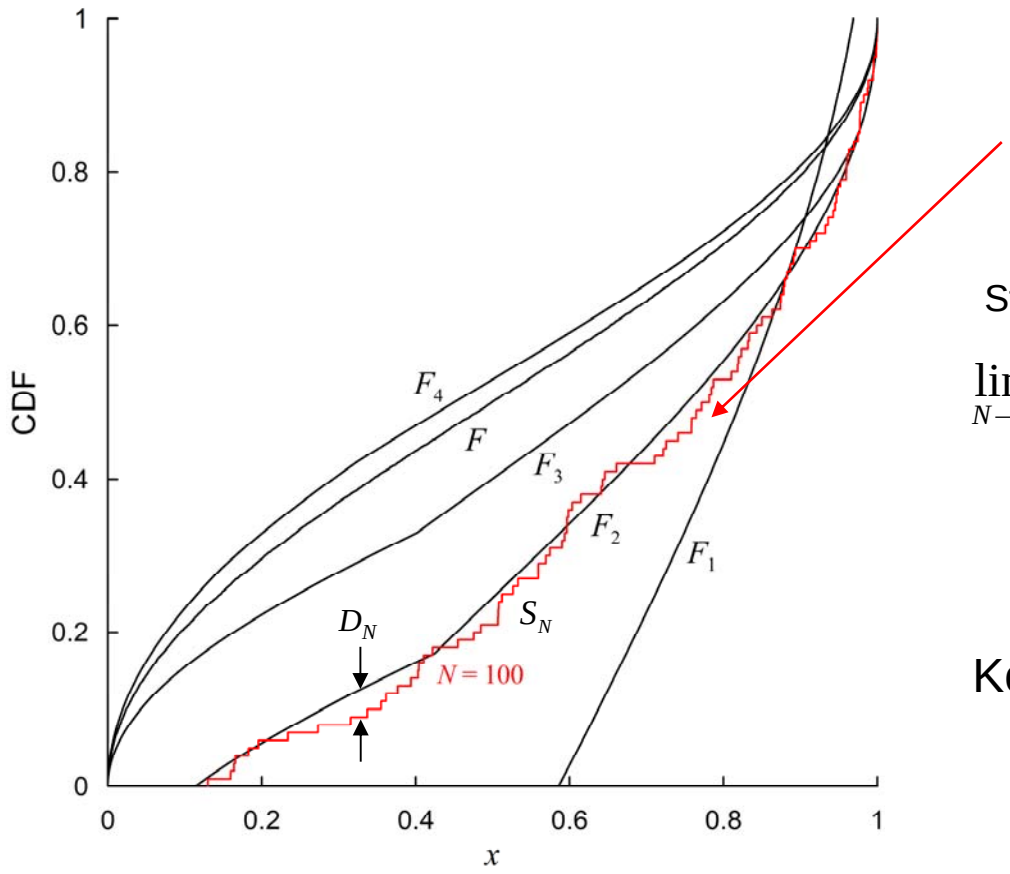

empirical CDF, $S_N(x)$

$$S_N(x) \equiv \begin{cases} 0, & x < x_1 \\ \dfrac{r}{N} & x_r < x < x_{r+1} \quad r = 1, \ldots, N-1 \\ 1 & x_N < x \end{cases}$$

Strong Law of Large Numbers:

$$\lim_{N \to \infty} S_N(x) = F(x)$$ (almost sure convergence)

Kolmogorov-Smirnov statistic, D_N

$$D_N \equiv \sup_x \left| S_N(x) - F_i(x) \right|$$

Sandia National Laboratories

Kolmogorov-Smirnov Statistic

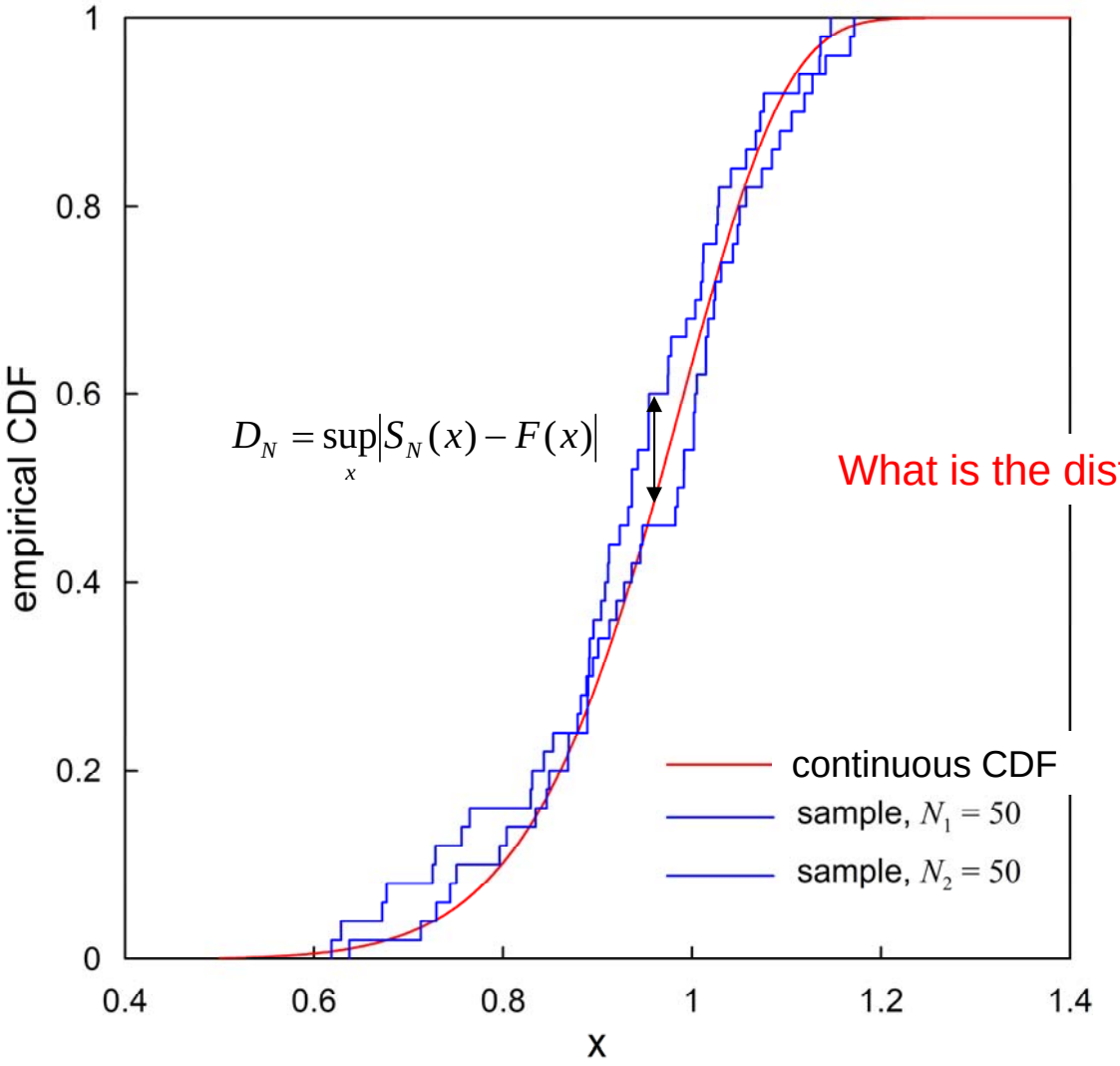

What is the distribution for D_N?

Sandia National Laboratories

Kolmogorov-Smirnov Statistic

A. KOLMOGOROV, *Sulla determinazione empirica di una legge di distribuzione*, Giornale dell'Istituto Italiano degli Attuari, 4 (1933), pp. 83–91.

$$D_N = \sup_x \left| S_N(x) - F(x) \right|$$

asymptotic result

$$\lim_{N\to\infty} \Pr(D_N < z/\sqrt{N}) = 1 - 2\sum_{j=1}^{\infty} (-1)^{j-1} \exp(-2j^2 z^2) \equiv p(z)$$

(convergence in probability)

(conservative to within 2% for $N > 50$)
(tabulated for $N < 50$)

- independent of distribution
- only for continuous CDFs
- gives confidence bounds

Sandia National Laboratories

Kolmogorov-Smirnov Statistic

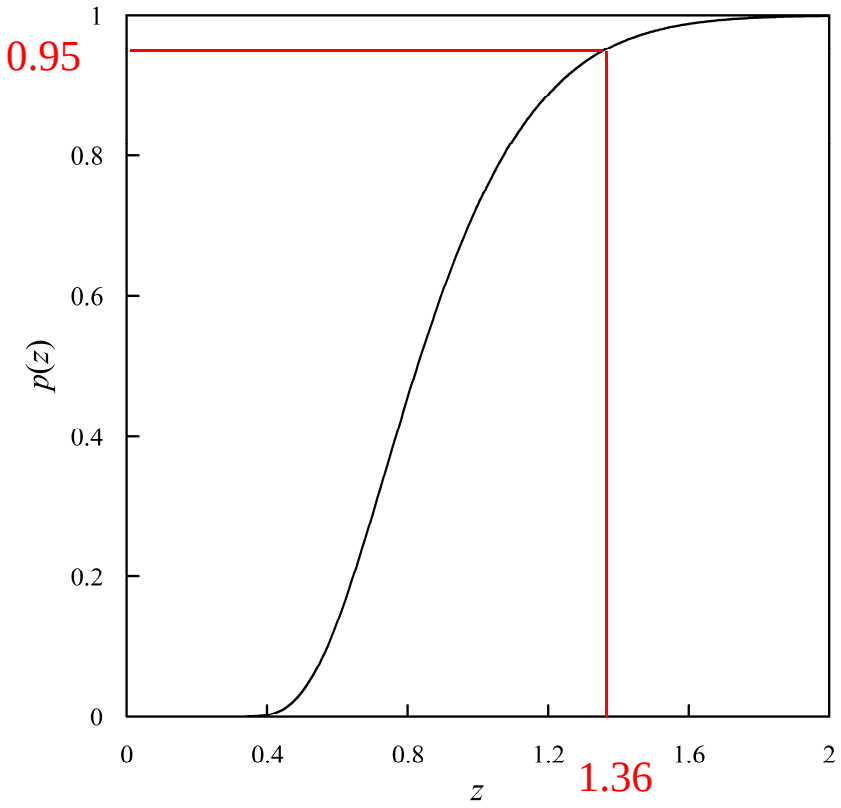

$$D_N = \sup_x \left| S_N(x) - F(x) \right|$$

$$\Pr\left(D_N < \frac{1.63}{\sqrt{N}} \right) = 99\%$$

$$\Pr\left(D_N < \frac{1.36}{\sqrt{N}} \right) = 95\%$$

$$\Pr\left(D_N < \frac{1.19}{\sqrt{N}} \right) = 90\%$$

(conservative to within 2% for $N > 50$)
(tabulated for $N < 50$)

Sandia National Laboratories

Kolmogorov-Smirnov Statistic

95% confidence bounds

$N = 50$

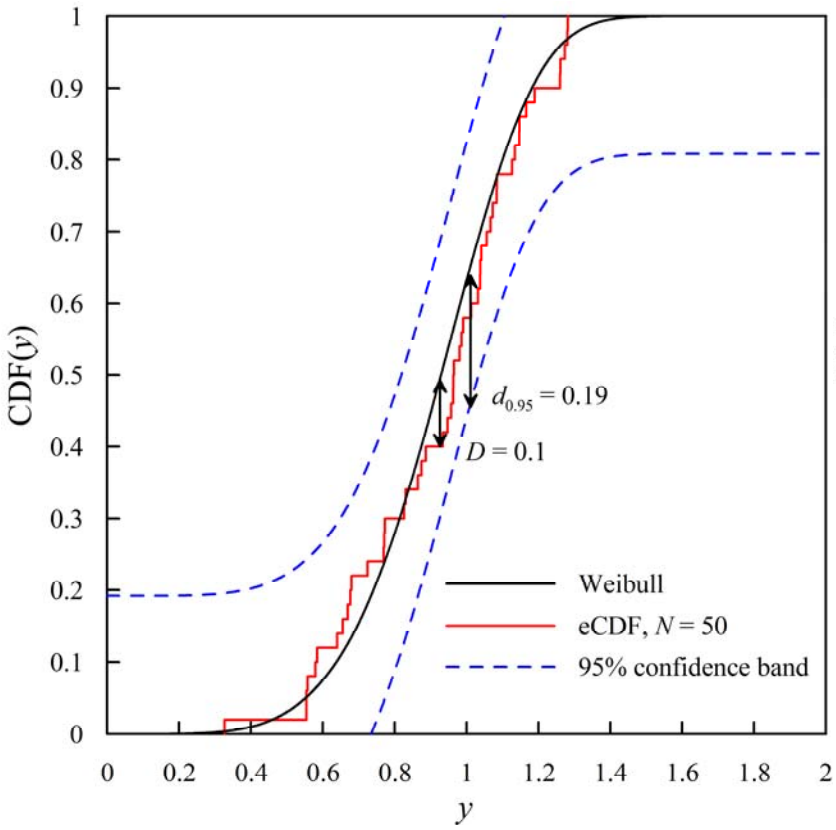

$N = 500$

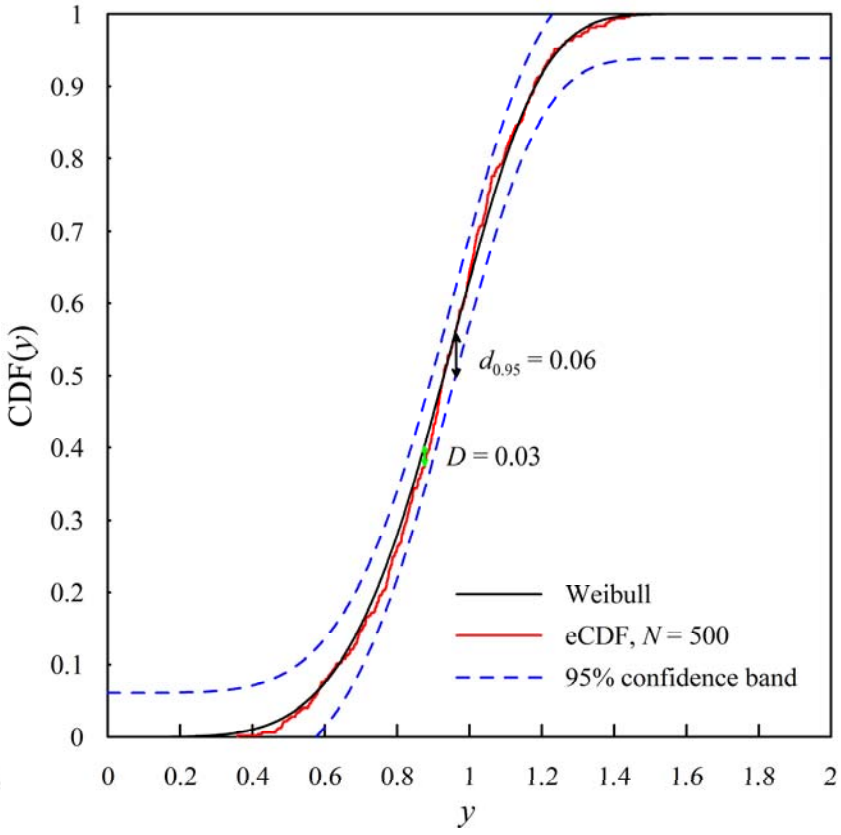

Sandia National Laboratories

How to use KS-statistic to assess convergence-in-distribution with finite sample sizes?

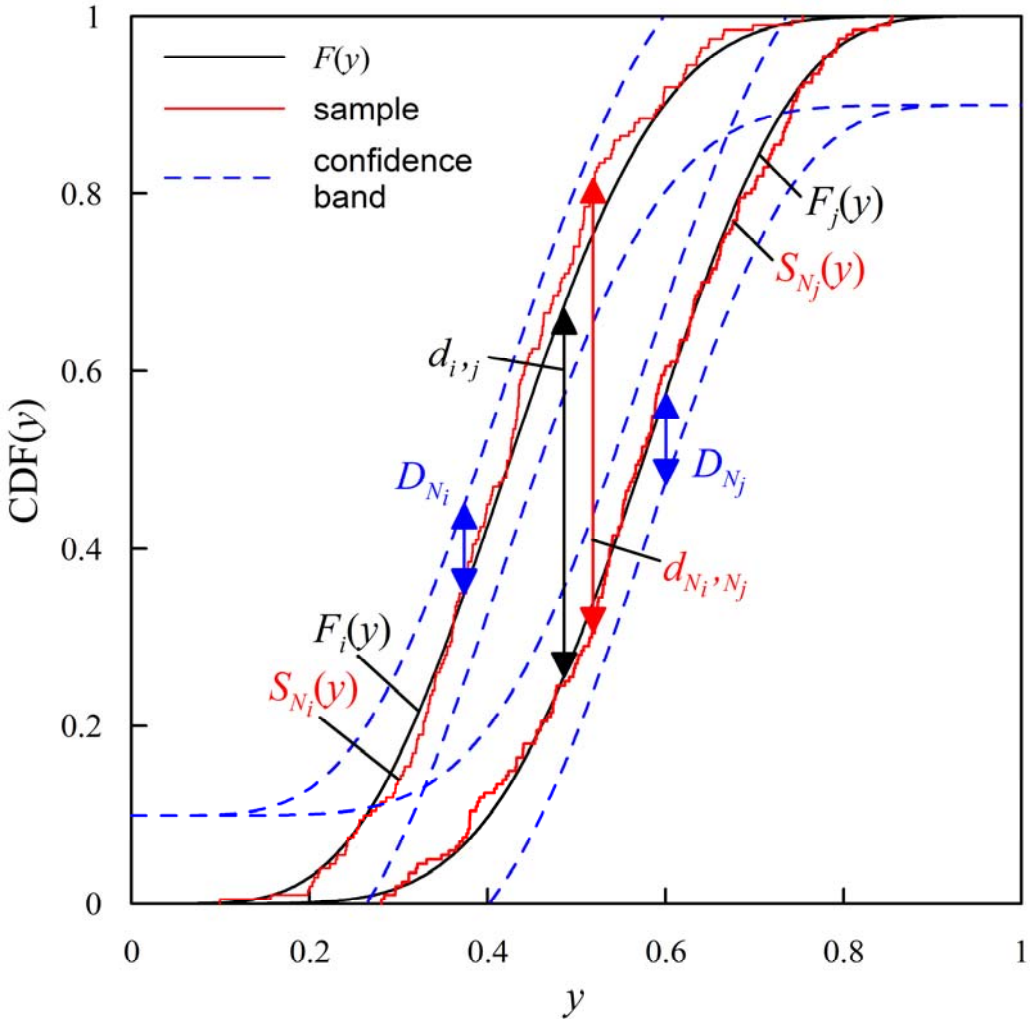

$$\left| d_{i.j} - d_{N_i,N_j} \right| \le D_{N_i} + D_{N_j} = \frac{z_i}{\sqrt{N_i}} + \frac{z_j}{\sqrt{N_j}}$$

Also, joint probability reduces confidence level.

Sandia National Laboratories

Simulation

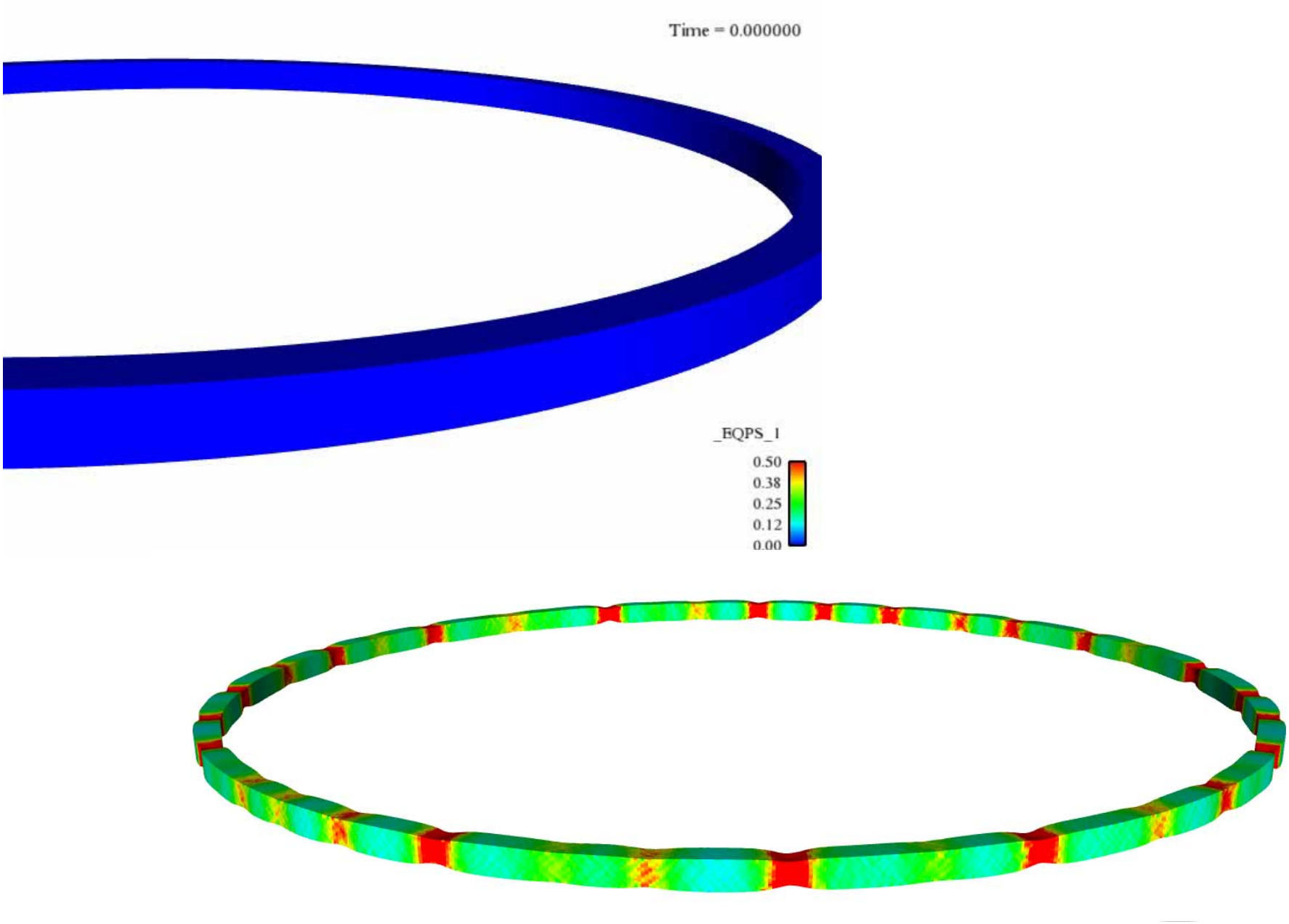

Four Mesh Refinement Levels

R0

- 6K elements
- 1 proc. on workstation
- ~10 min runtime

R1

- 48K elements
- 1 proc. on workstation
- ~2 hour runtime

R2

- 385K elements
- 16 proc. on tbird
- ~2 hour runtime

R3

- 3M elements
- 128 proc. on tbird
- ~4 hour runtime

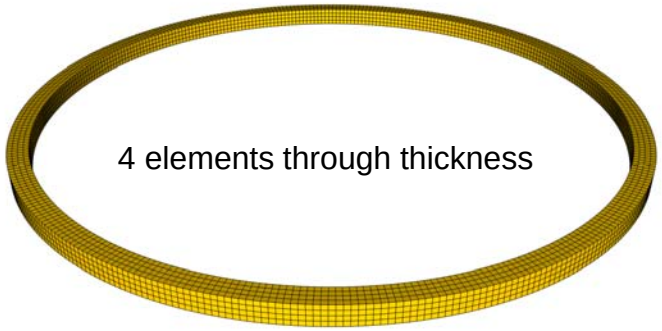

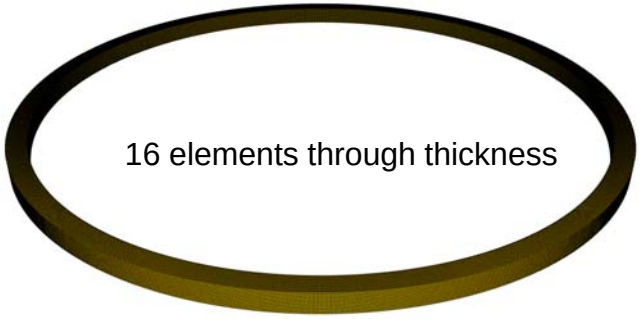

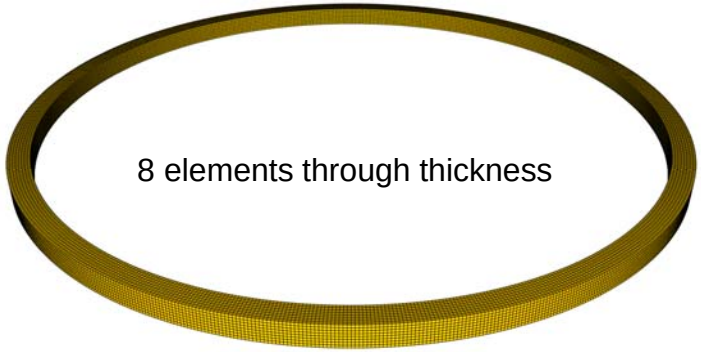

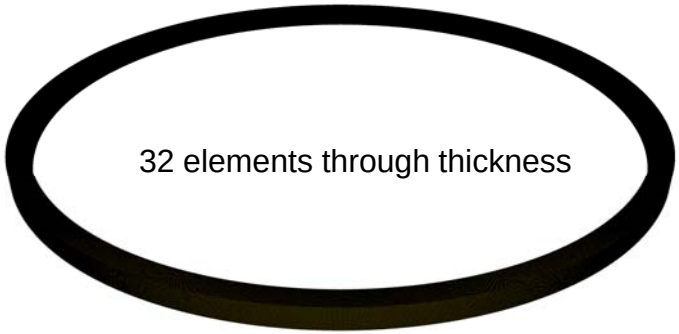

Sandia National Laboratories

Material Variability

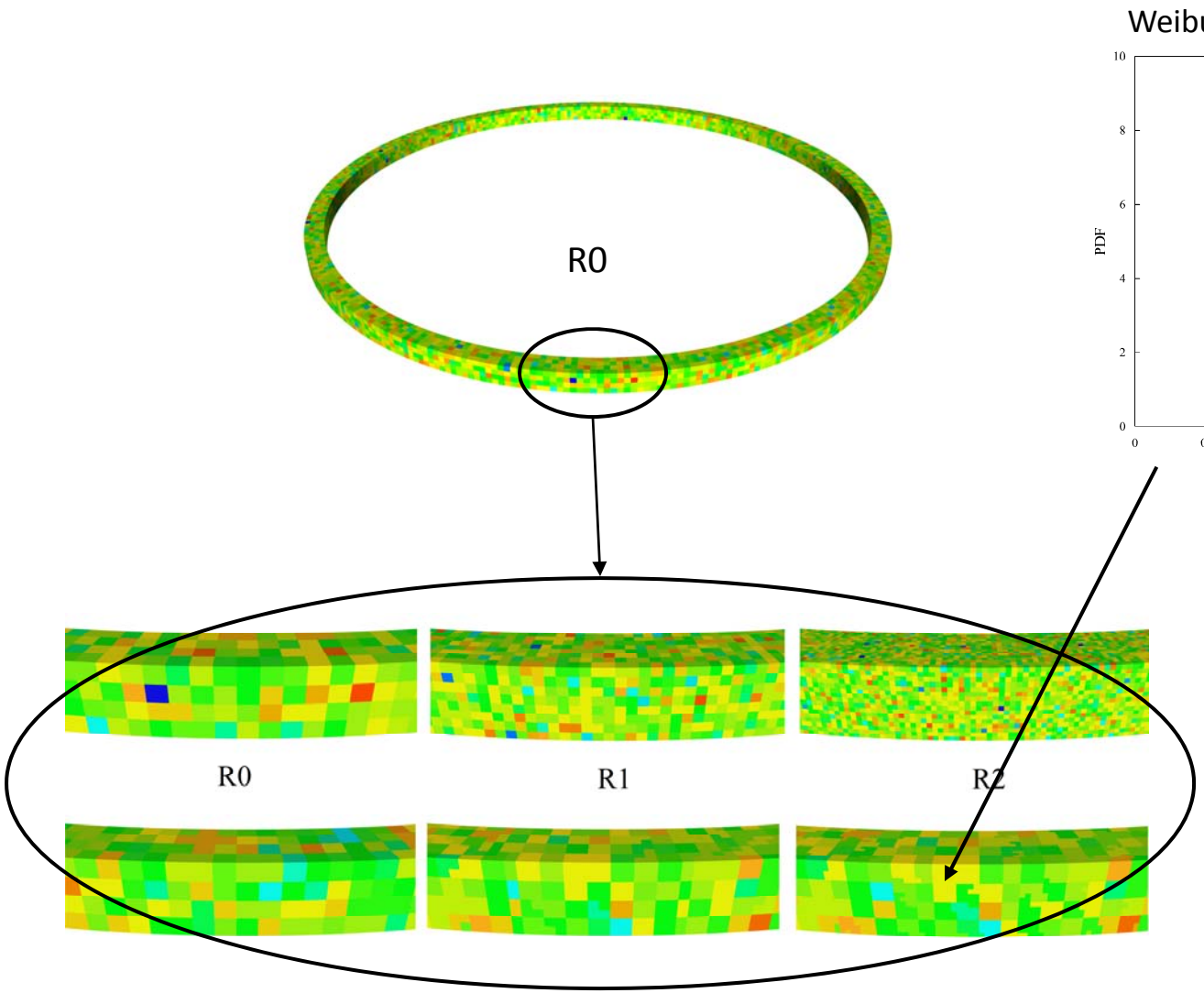

Weibull Probability Density

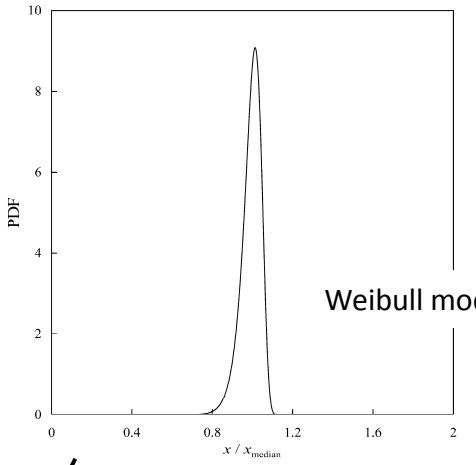

Weibull modulus = 25

without texture

each *element* is iid

(independent, identically distributed)

with texture

each "*cell*" is iid

Sandia National Laboratories

Cross-Sectional Area

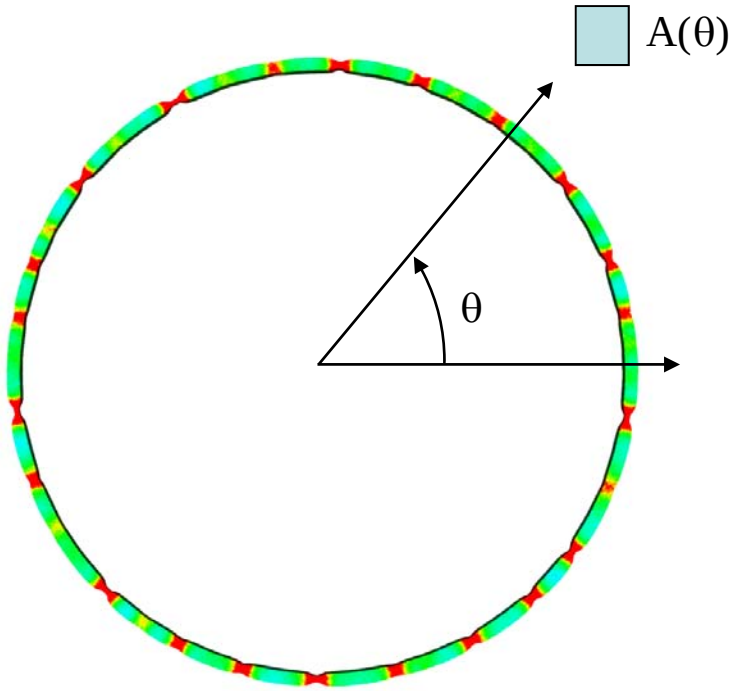

Reduce 3D random field to 1D random field.

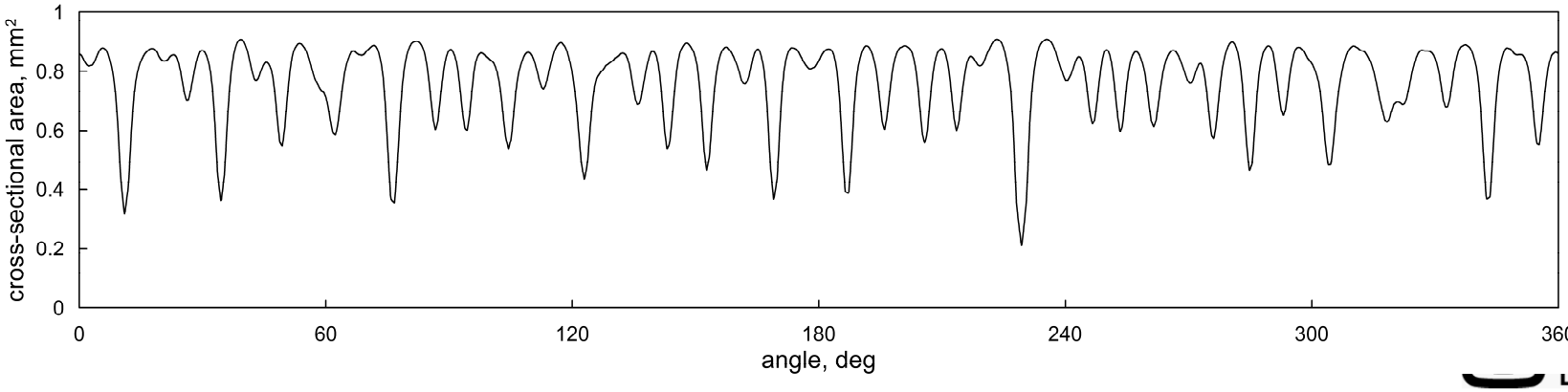

andia
ational
aboratories

Neck Identification

Sandia National Laboratories

Convergence in Distribution?

with material texture

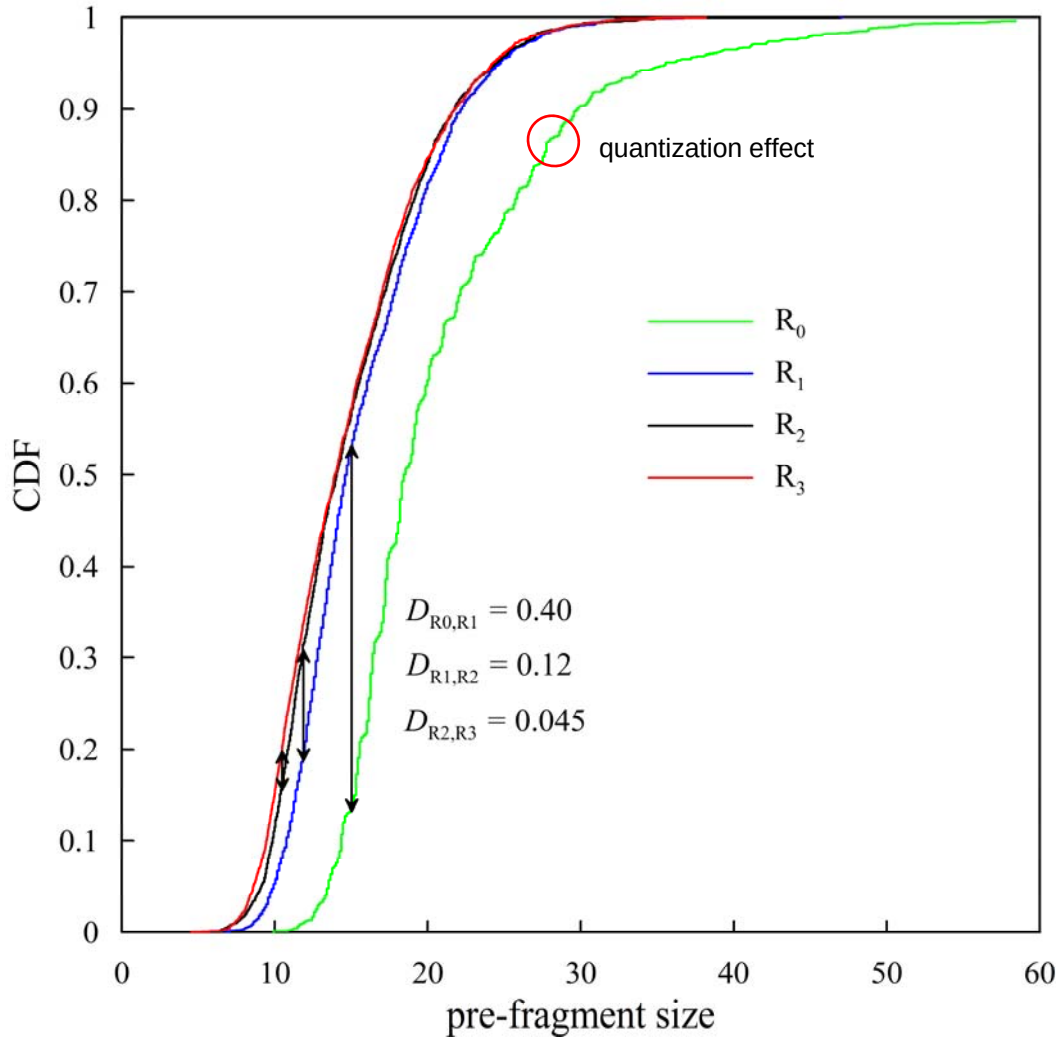

100 run ensemble

sample sizes

$N_0 = 1714$

$N_1 = 2274$

$N_2 = 2386$

$N_3 = 2421$

Warning: We have to be careful here. The KS statistic is predicated on simple random sampling. Combining multiple fragments from one simulation is cluster sampling.

Sandia National Laboratories

Quantization Error

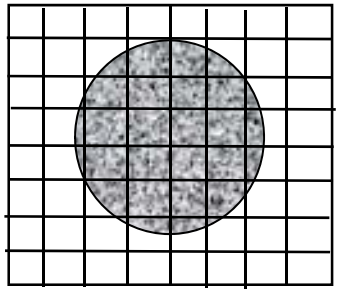

Fragment size is discretized to h in 1D.

Fragment size is discretized to h^2 in 2D.

Fragment size is discretized to h^3 in 3D.

$\lim_{N\to\infty} \mathrm{CDF}$ is not continuous.

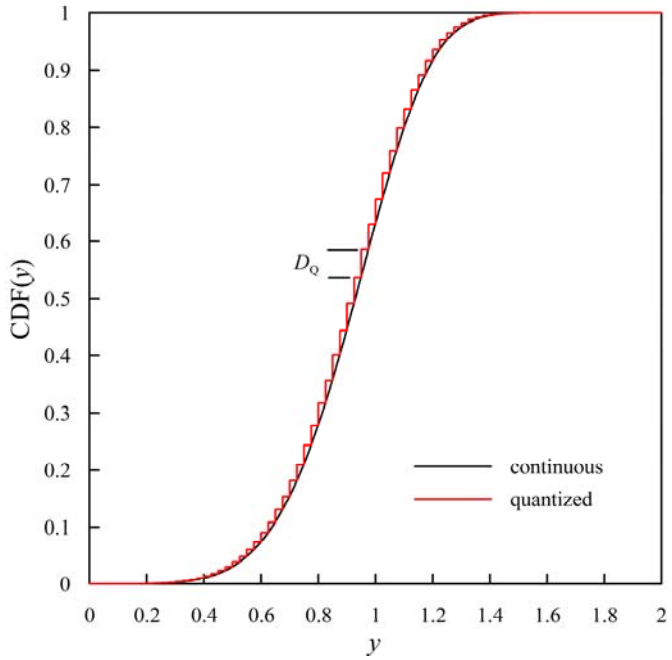

$$|d_{i,j} - d_{N_i,N_j}| \leq z_i/\sqrt{N_i} + z_j/\sqrt{N_j} + D_{Q_i} + D_{Q_j}.$$

$$D_Q = \max_{y\in\mathbb{R}} \left(\frac{dF}{dy}\right) \Delta y.$$

Sandia National Laboratories

Convergence in Distribution?

without material texture

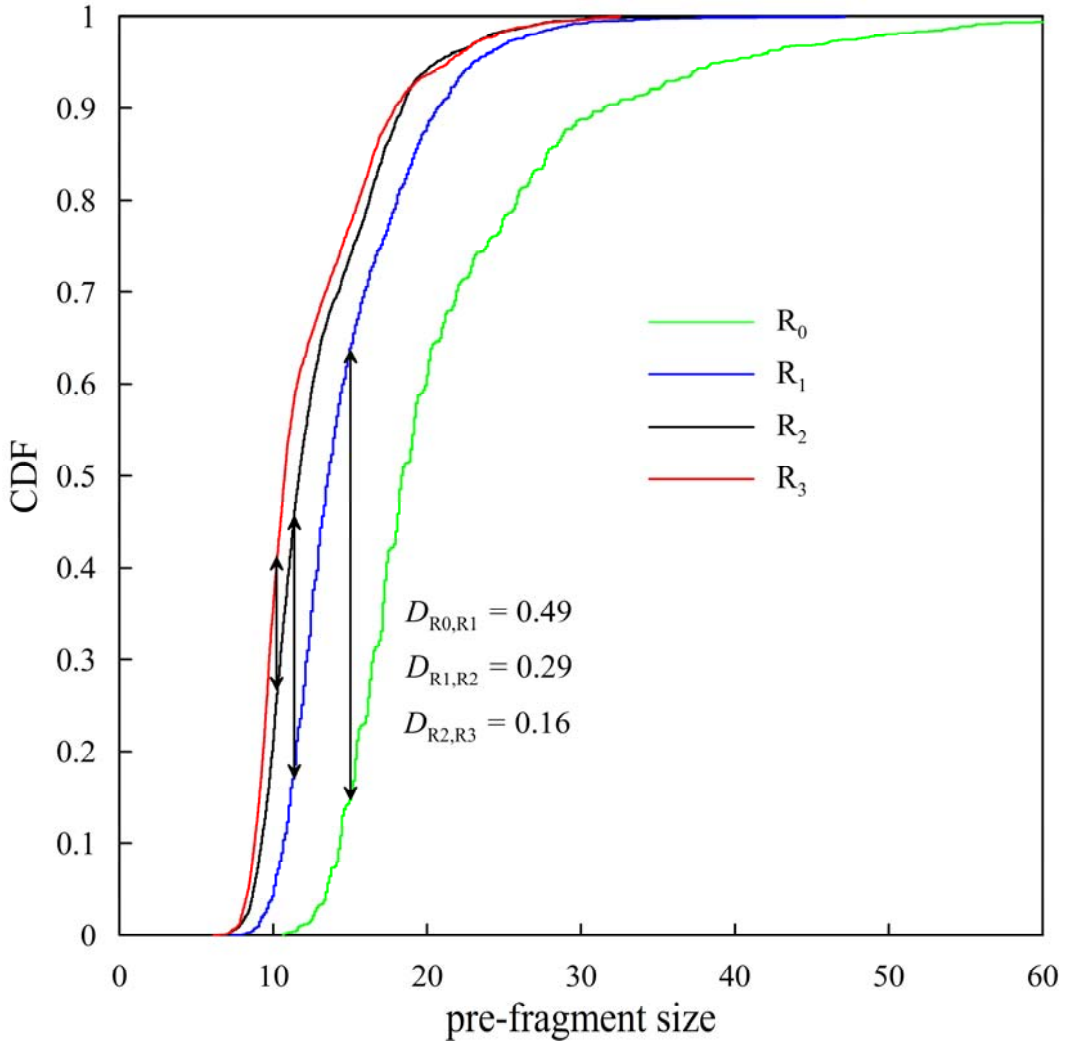

100 run MC ensemble

sample sizes

$N_0 = 1686$

$N_1 = 2424$

$N_2 = 2766$

$N_3 = 2905$

Sandia National Laboratories

Convergence in Distribution?

with material texture

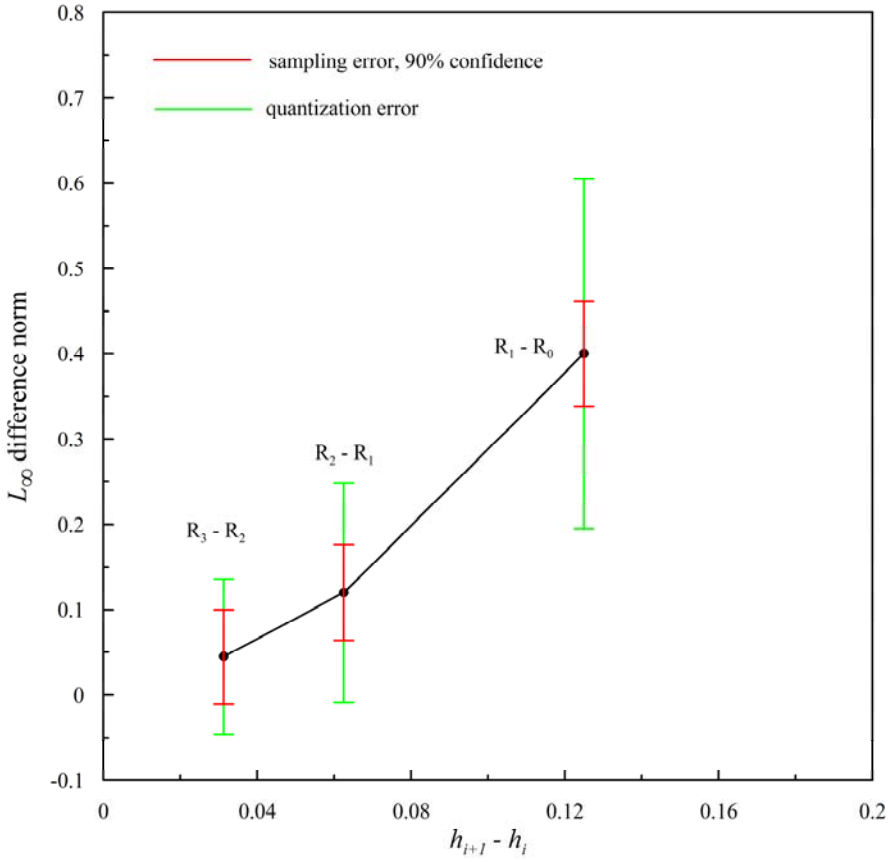

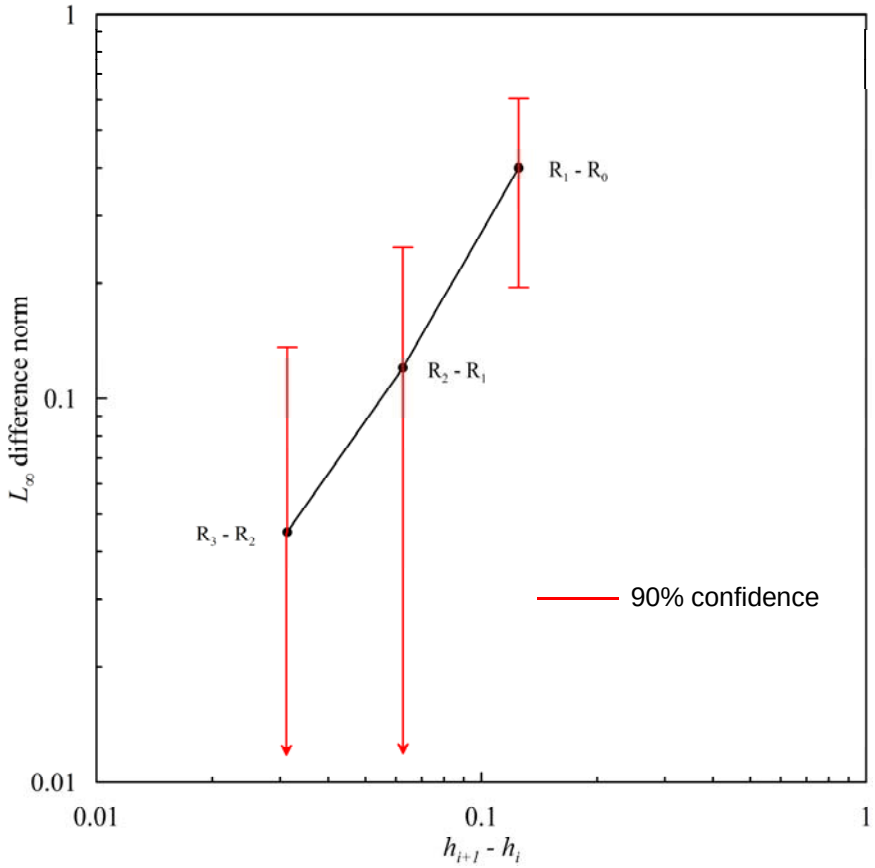

Sandia National Laboratories

Convergence in Distribution?

without material texture

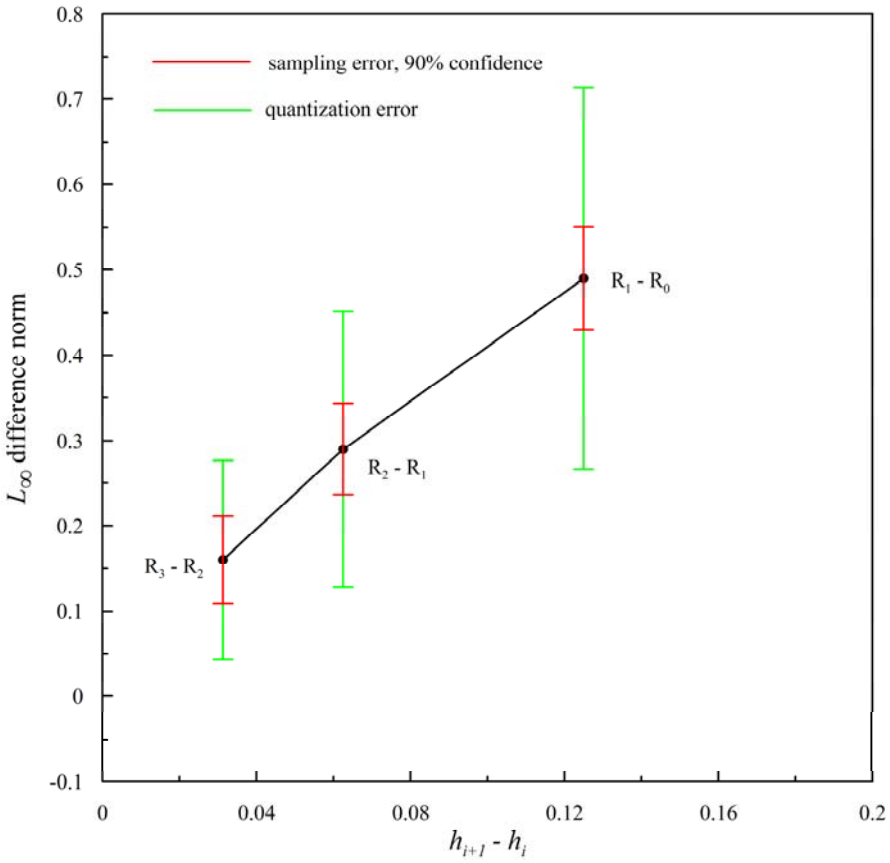

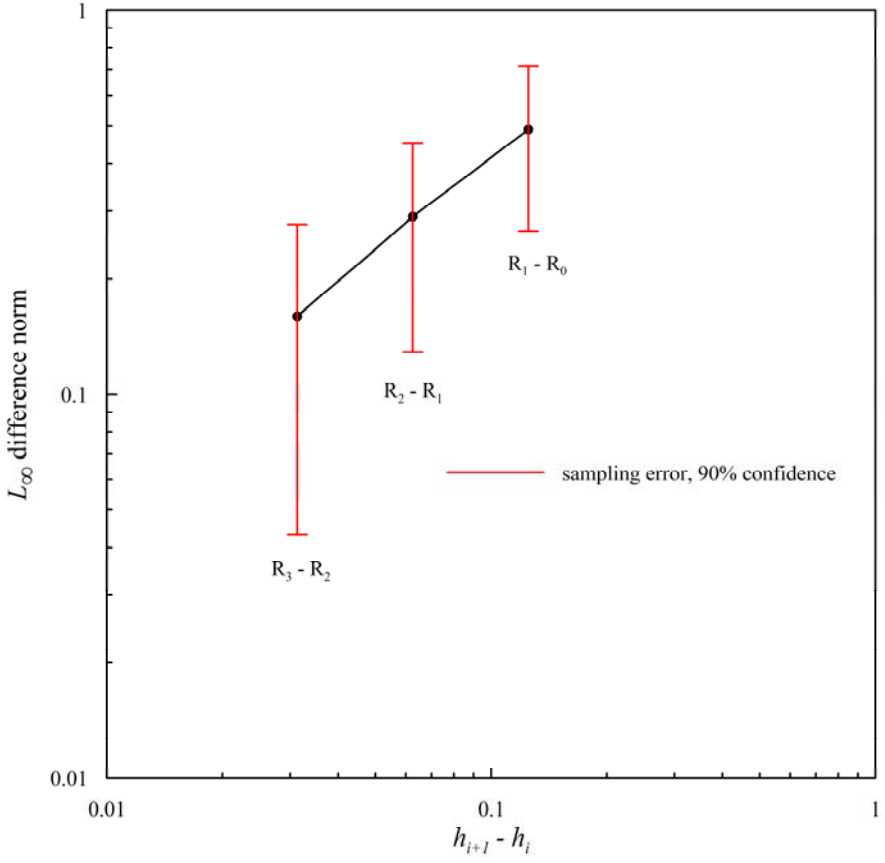

Sandia National Laboratories

Convergence in Distribution?

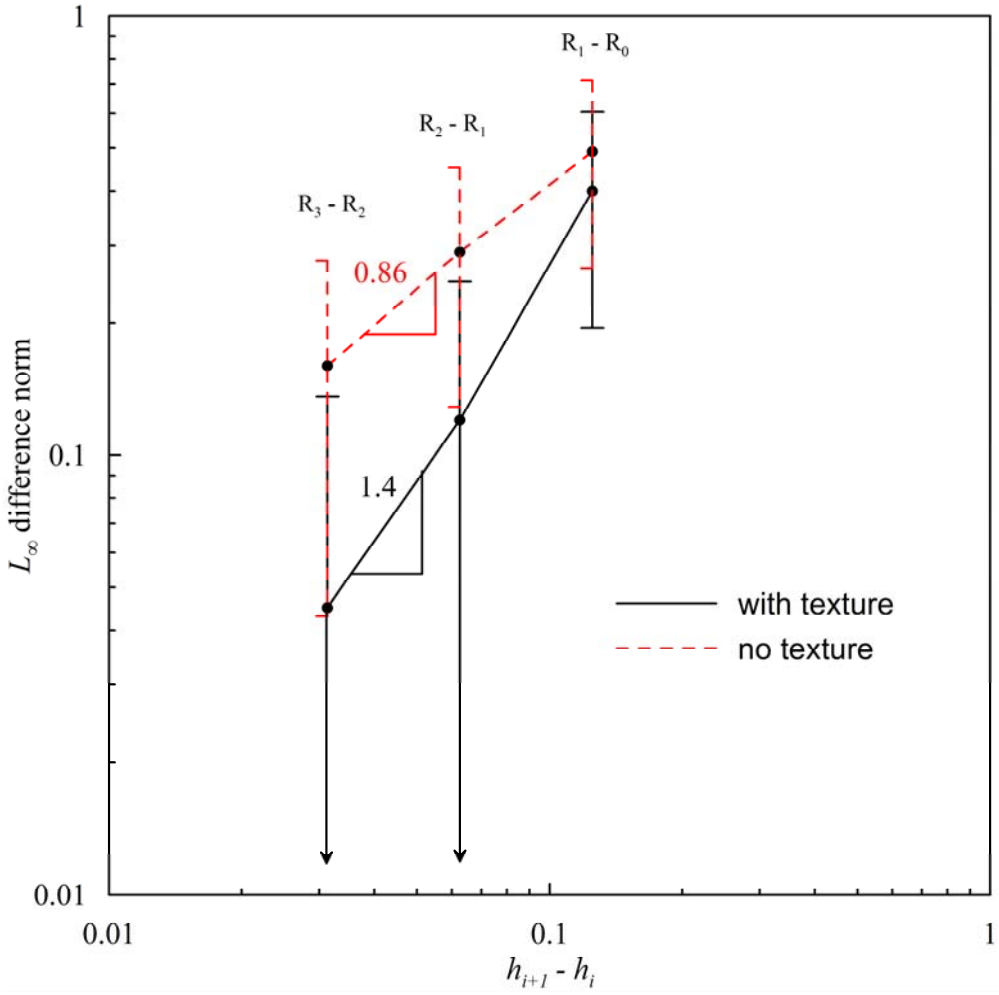

Sandia National Laboratories

Optimal Sample Sizes

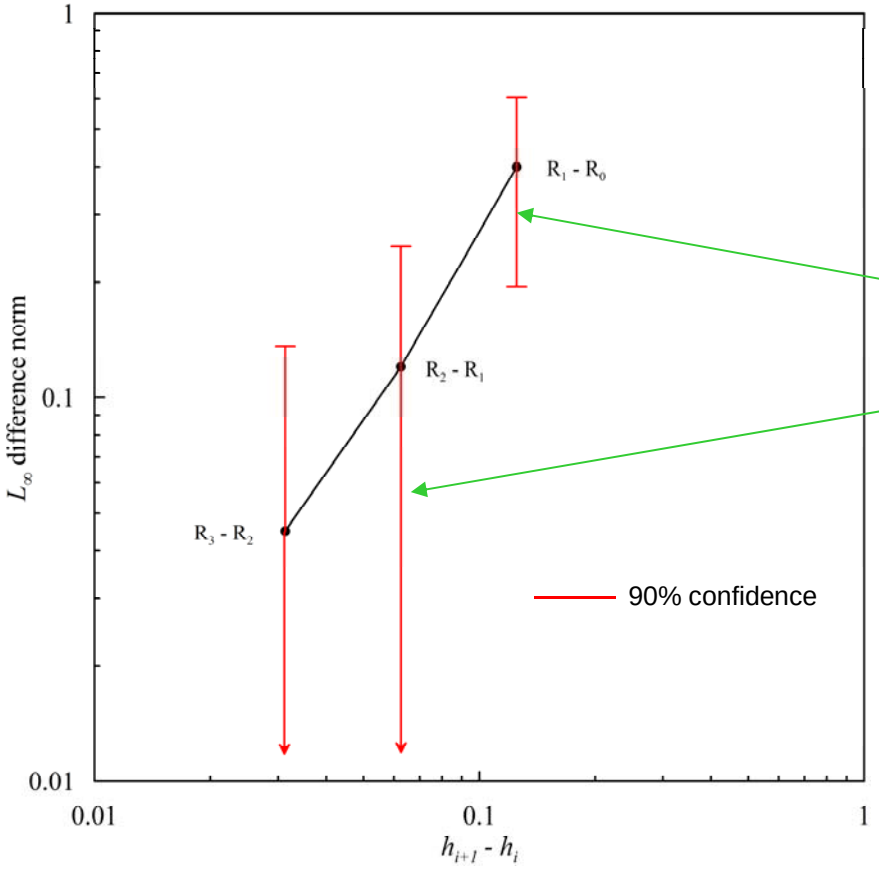

Need to increase sample size with mesh refinement to maintain a constant ratio of confidence-bound to error.

Sandia National Laboratories

Optimal Sample Sizes

Cost function $F_c(N_1, N_2, \ldots, N_n) := a_1 N_1 + a_2 N_2 + \cdots + a_n N_n$

Constraints $C_i(N_i, N_{i+1}) := \dfrac{z_i/\sqrt{N_i} + z_{i+1}/\sqrt{N_{i+1}}}{d_{i,i+1}} - \delta = 0, \quad i = 1, \ldots, n-1$

Augmented Lagrangian $L_A(N_1, \ldots, N_n, \lambda_1, \ldots, \lambda_{n-1}) := F_c(N_i) + \lambda_1 C_1 + \cdots + \lambda_{n-1} C_{n-1}$

Lagrange multipliers

Necessary conditions for an extremum $\dfrac{\partial L_A}{\partial N_i} = 0, \quad i = 1, \ldots, n$

Can show that Hessian matrix of L_a is positive definite, so the critical points are relative minima.

Sandia National Laboratories

Optimal Sample Sizes

$n-1$ equations for $n-1$ Lagrange multipliers

$$\left(\frac{\lambda_1}{2a_1z_1}\right)^{-1/3}+\left(\frac{\lambda_1+\lambda_2}{2a_2z_2}\right)^{-1/3}=\delta d_{1,2},$$
$$\left(\frac{\lambda_1+\lambda_2}{2a_2z_2}\right)^{-1/3}+\left(\frac{\lambda_2+\lambda_3}{2a_3z_3}\right)^{-1/3}=\delta d_{2,3},$$
$$\vdots$$
$$\left(\frac{\lambda_{n-3}+\lambda_{n-2}}{2a_{n-2}z_{n-2}}\right)^{-1/3}+\left(\frac{\lambda_{n-2}+\lambda_{n-1}}{2a_{n-1}z_{n-1}}\right)^{-1/3}=\delta d_{n-2,n-1},$$
$$\left(\frac{\lambda_{n-2}+\lambda_{n-1}}{2a_{n-1}z_{n-1}}\right)^{-1/3}+\left(\frac{\lambda_{n-1}}{2a_nz_n}\right)^{-1/3}=\delta d_{n-1,n}.$$

These equations “telescope” to give one nonlinear equation that can be solved numerically. Then, back substitute and solve for all λ.

Get optimal sample sizes at each mesh level.

$$N_1=\left(\frac{\lambda_1z_1}{2a_1}\right)^{2/3},$$
$$N_2=\left(\frac{(\lambda_1+\lambda_2)z_2}{2a_2}\right)^{2/3},$$
$$N_3=\left(\frac{(\lambda_2+\lambda_3)z_3}{2a_3}\right)^{2/3},$$
$$\vdots$$
$$N_{n-1}=\left(\frac{(\lambda_{n-2}+\lambda_{n-1})z_{n-1}}{2a_{n-1}}\right)^{2/3},$$
$$N_n=\left(\frac{\lambda_{n-1}z_n}{2a_n}\right)^{2/3}.$$

Sandia National Laboratories

Optimal Sample Sizes

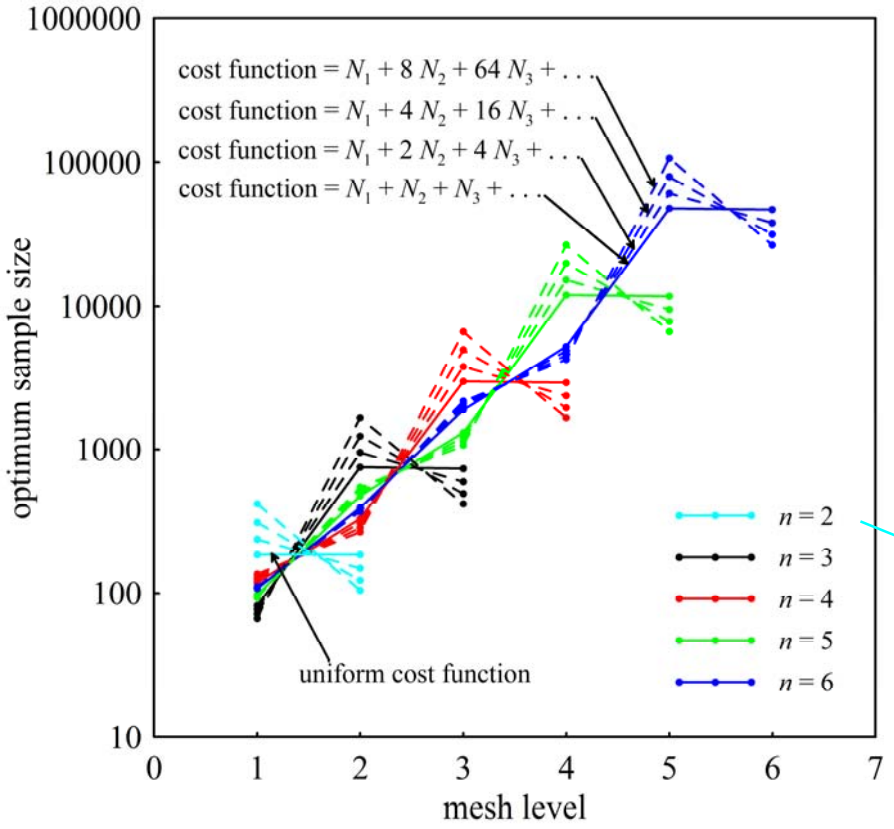

For two meshes we can solve explicitly.

$$N_1 = \frac{(z_1/2a_1)^{2/3}}{(\delta d_{1,2})^2}[(2a_1z_1)^{2/3} + (2a_2z_2)^{2/3}]^3,$$

$$N_2 = \frac{(z_2/2a_2)^{2/3}}{(\delta d_{1,2})^2}[(2a_1z_1)^{2/3} + (2a_2z_2)^{2/3}]^3.$$

Sandia National Laboratories

Optimal Sample Sizes

piece-wise linear approximations to a quadratic map

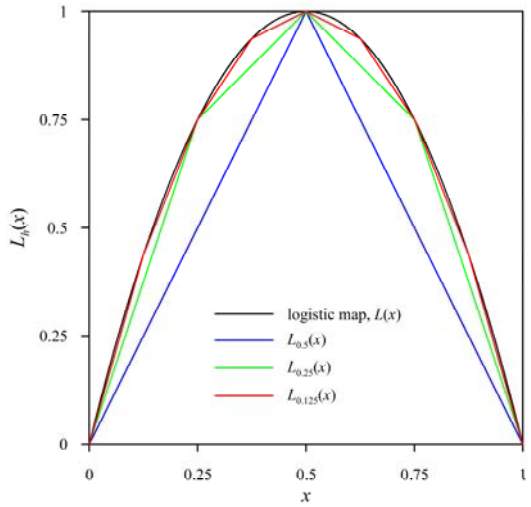

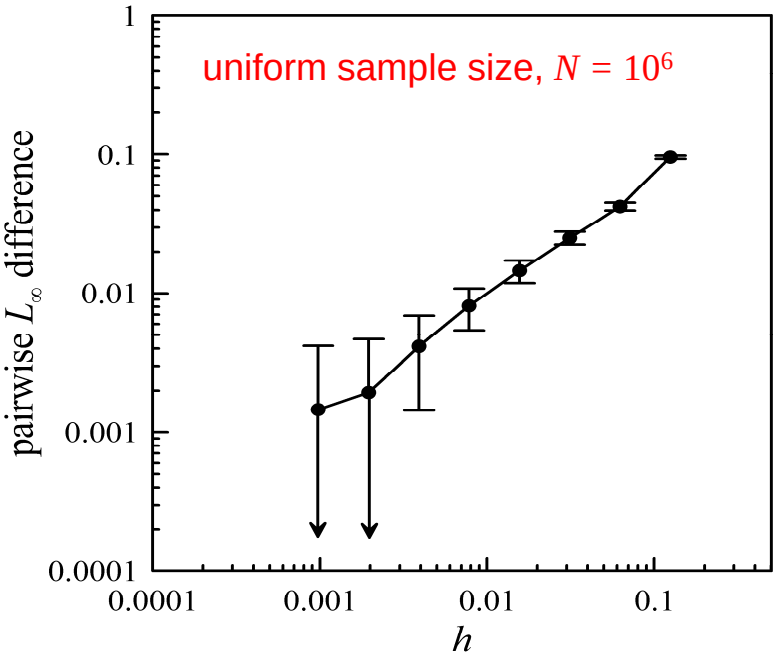

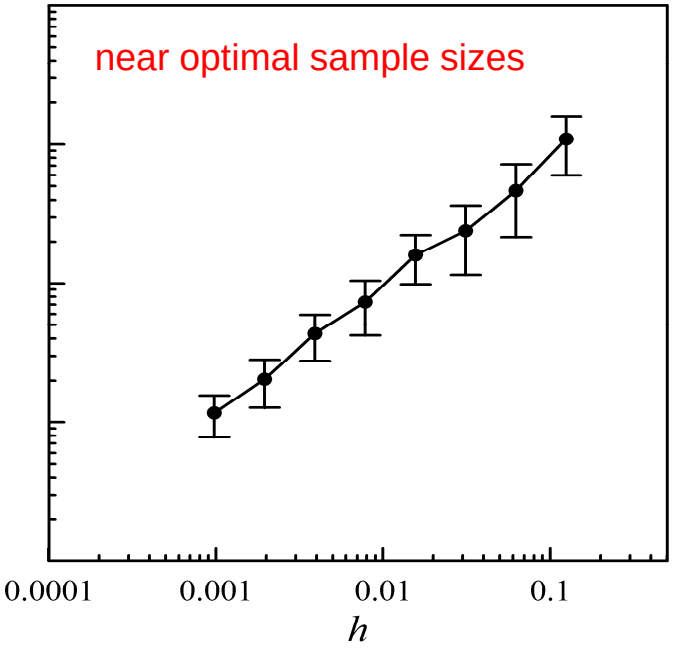

optimal sample sizes

$N_1 = 1660$
$N_2 = 6710$
$N_3 = 26 \times 10^3$
$N_4 = 110 \times 10^3$
$N_5 = 400 \times 10^3$
$N_6 = 1.94 \times 10^6$
$N_7 = 5.37 \times 10^6$
$N_8 = 49 \times 10^6$
$N_9 = 48 \times 10^6$

Sandia National Laboratories

Summary

1. Class of deterministic dynamical systems that are extremely sensitive to initial conditions.
2. For these systems, spectral methods and variance reduction methods are ineffective. Need to resort to direct Monte Carlo sampling.
3. Presented a method based on the KS-statistic to verify convergence in distribution with mesh refinement.
4. Presented a method for finding the optimal sample sizes at each mesh level for minimizing a linear cost function.